Colloid Polym Sci 274:439–445 (1996)

ORIGINAL CONTRIBUTION

B. Gerharz
R. Horst

Phase behavior of the ternary system water/hydroxyethyl cellulose/nonionic surfactant

Received: 2 November 1995
Accepted: 20 November 1995

Affectionately dedicated to Professor Dr. B.A. Wolf on the occasion of his 60th birthday.

B. Gerharz
Hoechst AG
65926 Frankfurt am Main, FRG

R. Horst (✉)
Johannes-Gutenberg-Universität Mainz
Institut für Physikalische Chemie
Jakob-Welder-Weg 13
55099 Mainz, FRG

Abstract The phase behavior of ternary aqueous solutions of two samples of hydroxyethyl cellulose (HEC) and oligoethylene glycol mono(*n*-alkyl) ethers C_xE_y (x: 11; y: 28, 40) at 25 °C has been studied above the CMC of C_xE_y. The influence of molar mass of HEC and the number of ethylene glycol units on the phase diagram has been investigated. Both binary systems water/HEC and water/C_xE_y are completely miscible. The ternary mixture of water/polymer/nonionic surfactant is homogeneous if the weight fraction of water is larger than 0.93, or else it can separate segregatively, i.e., HEC is enriched in one phase, the surfactant in the other. The theoretical description is based on an equation for the Gibbs energy of mixing which takes polar conformations into account. The phase diagrams are calculated by means of a new method which does not require the derivatives of the Gibbs energy of mixing.

Key words Hydroxyethyl cellulose – phase behavior – phase separation – polymer-surfactant-interaction – aqueous solution

Introduction

The phase behaviour of ternary mixtures consisting of a polymer and a surfactant in water as the common solvent [1, 2, 3] is of great technical interest. These systems are widely used in important fields of application, such as adhesives, cosmetics, foodstuffs, paints, pharmaceuticals and in emulsion polymerization processes. The use of water as a solvent is imposed by ecological considerations. Those mixtures are also of fundamental importance in the field of colloid and surface science. The phase behavior of water/surfactant/oil(*n*-alkanes) [4] is well known whereas only a few data exist for systems with a polymer as third component.

Already a binary solution of a surfactant in water shows an intricate phase diagram with multiple phenomena like the formation of micelles above the critical micelle concentration (CMC) and liquid crystalline phases at high concentrations of the surfactant [5]. In practical use mixtures of surfactants (ionic and/or nonionic) are often common.

Combinations of water soluble polymers (derivatives of cellulose, poly(vinyl alcohol), poly(vinyl pyrrolidone), dextrine, poly acids etc.) and nonionic or ionic surfactants (oligoethylene glycol mono(alkyl/aryl) ethers, *n*-alkyl/aryl sulphonates or sulphates etc.) are often used in technical applications. Often derivatives of cellulose are employed as the polymeric component since cellulose as a natural polymer exhibits great ecological advantages. The phase behavior of these derivatives in water is studied comprehensively [6, 7].

In the literature [8] phase diagrams of water/ethyl hydroxyethyl cellulose/oligoethylene glycol mono(*n*-dodecyl) ether are described. The theoretical treatment of these aqueous solutions is difficult since not only van der Waals interactions [9, 10] but also H-bonds and other polar interactions must be taken into account [11]. The subject of the present publication is to establish the miscibility behavior of the ternary system water/hydroxyethyl cellulose/oligoethylene glycol mono(*n*-alkyl) ether. This mixture is a typical example for a ternary aqueous solution of a water soluble polymer and a nonionic surfactant.

Experimental section

Substances

The polymeric components used and marked as HEC1 and HEC2 were unfractionated commercial samples of hydroxyethyl cellulose with the trade names Tylose H300 and Tylose H4000 (Hoechst AG, Frankfurt), respectively. The nonionic surfactants C_xE_y were oligoethylene glycol mono(*n*-alkyl) ethers with y around 28 and 40. The number of carbon atoms of the alkyl chain has a distribution in the range from 9 to 15, the content of C_{11} is more than 90%. C_xE_y were commercial types with a distribution of alkyl chains and of ethylene glycol oligomeric chains (Emulsogen EPN, Hoechst AG).

Methods

All experiments were carried out at 25 °C. Viscosities were measured with Ubbelohde capillary viscometers of type Micro 1 with a capillary diameter of 0.40 mm. The solutions of HEC in H_2O were prepared a day before use and stirred at room temperature. Before the measurements the solutions were filtered through 0.45 μm Millipore membrane filters. The running times were determined with the fully automatic apparatus "AVS 300" (both parts were supplied by Schott, Mainz, Germany) and, if necessary, corrected according to Hagenbach.

Light-scattering measurements in solutions of the surfactants in water were performed to detect the size of micelles above the CMC. We used static and dynamic light scattering to detect via correlation function and inverse Laplace transformation (Contin) the diffusion coefficient and particle size of the micelles as well as an apparent molar mass of the micelles via Zimm evaluation [12, 13]. An ALV DLS/SLS-5000 laser light scattering goniometer equipped with a Thorn-EMI photomultiplier and a single mode fiber receiver has been used. The instrument is capable of both absolute integrated scattered intensities and photon correlation measurements at different scattering angles. Toluene was used as a reference for computing the Rayleigh ratio. An ALV-800 transputer board and a multiple tau digital correlator in fast tau expansion has been used for measurements of intensity-time correlation functions. A frequency doubled Nd-YAG-laser (ADLAS DPY 32511) operating at a wavelength of 532 nm has been used. Necessarily, the refractive index increments (dn/dc) were measured using a PKL-DRI double beam differential refractometer of polymer laboratories at a wavelength of 532 nm and 21 °C.

The observed one- and two-phase regimes of the three discussed ternary mixtures have been examined in the following way: The chosen concentrations of HEC and C_xE_y were solved in water at 80 °C and stirred at this temperature for 2 h, then cooled down to room temperature and after 2 h standing at *RT* the phase state was determined visually.

Cloud points were determined by titration. Aqueous HEC solutions containing up to 5 wt.-% HEC were titrated with a 20 wt.-% C_xE_y solution under stirring until the first visually detectable turbidity occurred.

Coexistence experiments were carried out to determine tie lines. Different mixtures of H_2O, HEC and C_xE_y, corresponding to points inside the miscibility gap, were prepared in an Erlenmeyer flask: H_2O and HEC were mixed first and after several hours of stirring C_xE_y was added. The solutions were stirred at room temperature overnight and kept at 25 °C for several days allowing the system to phase separate. Sol and gel were then removed with syringe. After evaporation of the solvent in vacuum at 60 °C the H_2O content in the coexisting phases was determined gravimetrically. C_xE_y was extracted from the precipitate with a mixture of acetone/H_2O 2:1. Since acetone is a solvent for C_xE_y but not for HEC, it only dissolves the surfactant. Water is needed to make HEC swell, since otherwise C_xE_y cannot separate from HEC. After removing the C_xE_y-solution the swollen solid was dried as described above. The content of HEC and C_xE_y was determined gravimetrically.

Theoretical background

Karlström [11] described the phase behavior of poly(ethylene oxide) PEO and water using the Flory–Huggins theory [14]. In this theoretical approach all substances are divided into segments. Their number N can be calculated by dividing the molar volume of the component by the molar volume of the segment V_s. For the actual calculations V_s is set equal to the molar volume of water. Karlström took into consideration that the polymer can have different conformers. Two types of states of the polymer are distinguished, the parameter P gives the probability that a segment is found in one of the states which interact more favorably with the solvent (polar conformations) and $(1 - P)$ is the probability for the nonpolar conformations. In polar solvents like water P increases with the content of the solvent. The parameter F is given as the quotient of the probability of nonpolar and polar conformations. Karlström calculated a phase diagram with a lower critical solution temperature (LCST) of 354 K (and a upper critical solution temperature (UCST) of 867 K). This approach is the basis for the description of a ternary solution of a polymer and a surfactant in a common solvent [15]. If the concentration regime of interest lies far above the critical micelle concentration the number of nonmicellized surfactants is very small and they can therefore be neglected in the theoretical approach. The micelle itself can be treated as a second polymer. The Gibbs energy of mixing per mol of segments reads

$$\begin{aligned}\frac{\overline{\overline{\Delta G}}}{RT} = {} & \varphi_1 \varphi_2[P_2\chi_{12\mathrm{p}} + (1-P_2)\chi_{12\mathrm{u}}] \\ & + \varphi_1 \varphi_3[P_3\chi_{13\mathrm{p}} + (1-P_3)\chi_{13\mathrm{u}}] \\ & + \varphi_2(1-P_2)\{\varphi_2 P_2\chi_{2\mathrm{p}2\mathrm{u}} + \varphi_3[P_3\chi_{2\mathrm{u}3\mathrm{p}} \\ & + (1-P_3)\chi_{2\mathrm{u}3\mathrm{u}}]\} \\ & + \varphi_2 P_2 \varphi_3[P_3\chi_{2\mathrm{p}3\mathrm{p}} + (1-P_3)\chi_{2\mathrm{p}3\mathrm{u}}] \\ & + \varphi_3\varphi_3 P_3(1-P_3)\chi_{3\mathrm{u}3\mathrm{p}} + \varphi_2^2(1-P_2)^2\frac{\chi_{2\mathrm{u}2\mathrm{u}}}{2} \\ & + \varphi_3^2(1-P_3)^2\frac{\chi_{3\mathrm{u}3\mathrm{u}}}{2} + \varphi_1\ln\varphi_1 \\ & + \frac{\varphi_2}{N_2}\ln\varphi_2 + \frac{\varphi_3}{N_3}\ln\varphi_3 \\ & + \varphi_2\left\{P_2\ln P_2 + (1-P_2)\ln\left[\frac{(1-P_2)}{F_2}\right]\right\} \\ & + \varphi_3\left\{P_3\ln P_3 + (1-P_3)\ln\left[\frac{(1-P_3)}{F_3}\right]\right\} \end{aligned} \tag{1}$$

where φ_i is the volume fraction of component *i*. The index 1 is used for the solvent (water), 2 for the polymer (HEC), 3 for the surfactant (C_xE_y). The parameters *P* and *F* occur for both polymeric substances.

The values of F_2 and F_3 are fixed as 8 [15], P_1 and P_2 are determined by the condition

$$\overline{\overline{\Delta G}}(P_1, P_2) = \min\ . \tag{2}$$

Since the minimum is found by iteration, the normal tools of thermodynamics cannot be applied to calculate phase diagrams since they require the derivatives of the Gibbs energy. The authors of ref. [15] only calculated tie lines giving the compositions of the coexisting phases, and so the binodal line, connecting the endpoints of all tie lines, with the aid of a Monte Carlo technique.

In this paper, a new method [16, 17] is employed which allows the calculation of the spinodal line, i.e., the border of the unstable area, and of critical points. The method only requires the knowledge of the Gibbs energy of mixing, but not its derivatives. For the calculation of tie lines, i.e., the composition of the coexisting phases, the condition is used that the Gibbs energy of mixing of the whole heterogeneous system must be minimum. For the determination of the stability of the mixture it is assumed that the system demixes into two phases with a composition very similar to that of the overall system. This test demixing should not be confused with the equilibrium situation of a two-phase system. The two new phases are not coexisting phases, they are just hypothetical states. For each component the volume fractions of the two phases differ from the overall value by the same amount, i.e., the overall composition is located exactly in the middle of the test tie line. One additional parameter is required to describe exactly the test demixing since one degree of freedom is left applying the above conditions for ternary systems. The value of this parameter can be found numerically by the condition that $\Delta G^{\pm}$, the Gibbs energy of the overall system consisting of the two test phases, must be minimum. If $\Delta G^{\pm}$ for a given overall composition is lower than ΔG of the homogeneous overall system the mixture is unstable, if $\Delta G^{\pm}$ is larger the mixture is (meta) stable. For $\Delta G^{\pm} = 0$ the overall composition is located on the spinodal line. The critical point is defined by the condition that the end points of the test tie line must be located on the spinodal line.

Equation (1) contains twelve interaction parameters χ_{ij}. The indices 1, 2, and 3 give the interacting components, and the subscripts *u* and *p* mark the polar or nonpolar conformation of the substance. The interaction of segments of the same component in the nonpolar state, $\chi_{2\mathrm{u}2\mathrm{u}}$ and $\chi_{3\mathrm{u}3\mathrm{u}}$, must also be included in order to describe the equilibrium between the polar and nonpolar states.

The temperature dependence of the interaction parameters is assumed to be

$$\chi_{ij} = \frac{\omega_{ij}}{RT} \tag{3}$$

with ω_{ij} and *T* being a temperature independent parameter and the temperature, respectively. For the determination of these interaction parameters we follow the procedure described in reference [15]. First the four interaction parameters of each binary system solvent/polymer are modeled. Therefore the LCST of H_2O/PEO for the given segment number is calculated. Dividing ω_{ij} for H_2O/PEO by this LCST and multiplying with the actual LCST gives the values for the actual binary mixture. So eight interaction parameters are fixed by assuming the two LCSTs for the binary subsystems. The remaining parameters $\omega_{2\mathrm{p}3\mathrm{p}}, \omega_{2\mathrm{u}3\mathrm{p}}, \omega_{2\mathrm{p}3\mathrm{u}}$, and $\omega_{2\mathrm{u}3\mathrm{u}}$ are used to model phase diagrams or are determined by fitting the binodal line to the observed cloud point curve or tie lines, respectively. This means that six parameters are required to describe the phase diagram.

Results and discussion

At the beginning the new calculation procedure [16, 17] was checked by recalculating some phase diagrams of ref. [15]. Figures 1 and 2 show the results for the ternary system II of Fig. 6 of ref. [15]. Interaction parameters are given in Table 1.

The binary system solvent/polymer exhibits a LCST at 334 K and the mixture solvent/surfactant a LCST at 320 K, i.e., all subsystems in Figs. 1 and 2 are completely miscible, except for solvent/surfactant at 330 K (Fig. 2). A closed miscibility gap exists at the lower temperature, the tie lines run nearly parallel to the subsystem polymer/surfactant, i.e., the polymer is enriched in one phase and the surfactant in the other. This phenomenon is called segregative phase separation [18]. Two critical points are found at this temperature. There are some slight deviations from Fig. 6a of reference [15]: The authors calculated a smaller miscibility gap, the system is homogeneous near the corner of the solvent whereas the ternary mixture is phase separated according to the actual calculations. The determination of the heterogeneous region in reference [15] is exclusively based on calculated tie lines. In the present Fig. 2 tie lines, spinodal line, and critical points are shown. All these results fit well together indicating that the actual calculations are correct. At 330 K the subsystem solvent/surfactant is demixed and therefore one calculates only one critical point. This phase diagram is identical with that of Fig. 6b of reference [15].

For the calculation of phase diagrams for the system $H_2O/HEC/C_xE_y$ the molar masses of the components (HEC and the micelles of C_xE_y) are required. For this purpose the intrinsic viscosities $[\eta]$ of HEC in water have been measured as described above. The viscometric results are shown as Huggins plots [19] in Fig. 3, Table 2 gives the values of $[\eta]$.

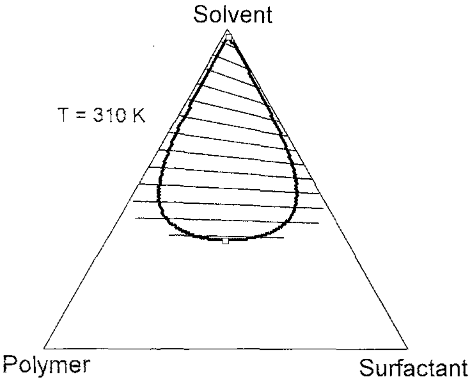

Fig. 1 Tie lines (solid lines), spinodal line (full circles), and critical points (open squares) for the ternary system of a solvent and two polymers of the same segment number $N_i = 20000$, $T = 310$ K and interaction parameters given in Table 1

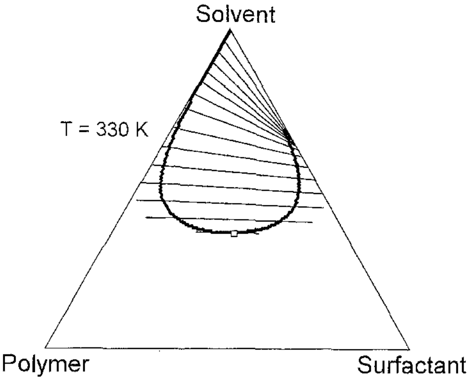

Fig. 2 Same graph as Fig. 1 for $T = 330$ K

The evaluation of intrinsic viscosities and molar masses determined by light scattering for HEC in water [20]

Table 1 Interaction parameters

<table>
<tr><th></th><th>H_2O/PEO</th><th>Model system</th><th>$H_2O/HEC/C_xE_{28}$</th><th>$H_2O/HEC/C_xE_{40}$</th></tr>
<tr><td>ω_{12p}</td><td>650.8</td><td>548.3</td><td colspan="2">737.7</td></tr>
<tr><td>ω_{12u}</td><td>10 654</td><td>9 590</td><td colspan="2">12 075</td></tr>
<tr><td>ω_{2p2u}</td><td>6 352</td><td>5 742</td><td colspan="2">7 199</td></tr>
<tr><td>ω_{2u2u}</td><td>10 172</td><td>9 195</td><td colspan="2">11 529</td></tr>
<tr><td>ω_{13p}</td><td></td><td>588.3</td><td colspan="2">1 106</td></tr>
<tr><td>ω_{13u}</td><td></td><td>9 630</td><td colspan="2">18 109</td></tr>
<tr><td>ω_{3p3u}</td><td></td><td>5 742</td><td colspan="2">10 797</td></tr>
<tr><td>ω_{3u3u}</td><td></td><td>9 195</td><td colspan="2">17 290</td></tr>
<tr><td>ω_{2p3p}</td><td></td><td>0</td><td colspan="2">75</td></tr>
<tr><td>ω_{2u3p}</td><td></td><td>5 742</td><td>6 200</td><td>6 097</td></tr>
<tr><td>ω_{2p3u}</td><td></td><td>5 742</td><td>6 200</td><td>6 097</td></tr>
<tr><td>ω_{2u3u}</td><td></td><td>9 195</td><td colspan="2">92 000</td></tr>
</table>

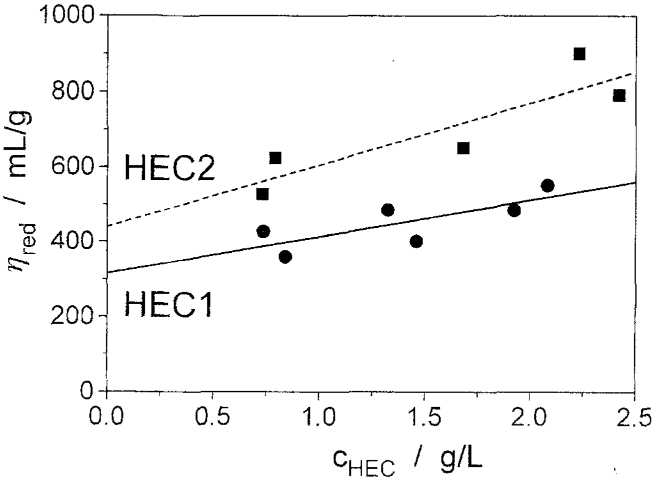

Fig. 3 Huggins plot for hydroxyethyl cellulose in water at 25 °C

Table 2 Intrinsic viscosity $[\eta]$, molar mass M, density ρ and number of segments N at 25 °C

	$[\eta]$/mL/g	M/kg/mol	ρ/g/cm^3	N
H_2O		$18.015\ 10^{-3}$	0.99707	1
HEC1	315	157	1.38965	6250
HEC2	440	229		9120
C_xE_{28} micelles		51	1.1135	2530
C_xE_{40} micelles		170	1.1307	8320

at 25 °C yields the following Kuhn–Mark–Houwink-equation

$$[\eta] = 0.00746\ \text{mL/g}\ (M/(\text{g/mol}))^{0.89}\ . \qquad (4)$$

The molar masses for the two HEC-samples can be calculated from the intrinsic viscosities, the M-values are given in Table 2.

The properties of C_xE_y in solution were determined by light scattering. The dn/dc-values for C_xE_y have been measured as 0.131 mL/g for C_xE_{28} and 0.132 mL/g for C_xE_{40}. From Zimm-evaluation one can calculate an apparent molar mass M_w of the micelles which yields 51 kg/mol for C_xE_{28} and 170 kg/mol for C_xE_{40}. Therefore we assume a coordination number of roughly 35 in the case of C_xE_{28} and 85 for C_xE_{40}. The second virial coefficient A_2 yields 6.6 10^{-4} mol cm^3/g^2 in the case of C_xE_{28} and 1.5 10^{-4} mol cm^3/g^2 for C_xE_{40}. From dynamic light scattering measurements one can determine the Stokes radius of the diffusing micelles in principle. We have used these experiments to prove the purity of the samples and the homogeneity in the concentration range of present interest. The critical micelle concentration is 1.6 g/L in the case of C_xE_{28} and 3.1 g/L for C_xE_{40} determined by surface tension measurements [21].

Knowing the molar masses of the components and their densities, one can calculate the segment numbers for each component (N_{H_2O} was set to unity). Table 2 gives the values for all substances under investigation.

At first the interaction parameters determining the mixing behavior for the binary systems H_2O/HEC and H_2O/C_xE_y have to be fixed. Both systems are completely miscible in the whole experimentally accessible temperature range up to 100 °C. So the LCST must be larger than this value.

Four interaction parameters describing the interaction between the polymer and the surfactant remain: The two parameters ω_{2u3p} and ω_{2p3u} were fixed to a value of 6000 J/mol similar to that used in ref. [15]. ω_{2p3p} describing the interactions of segments in the polar conformations must be very small since the homogeneous region in the solvent corner of the phase diagram is very large and the polar conformations predominate here. The opposite holds for ω_{2u3u} since the binary subsystem HEC/C_xE_y is highly incompatible.

In order to describe the measured cloud point curves and tie lines a LCST of 400 K for H_2O/HEC and 600 K for H_2O/C_xE_y seemed to be a good choice. Naturally it cannot be expected that the simple temperature dependence of Eq. (3) holds for a temperature interval of more than 100 °C. The LCSTs have no real physical meaning, they are just parameters to describe the behavior at 25 °C. The parameters ω_{2p3p} and ω_{2u3u} were varied, until the theoretical binodal and tie lines fitted well the experimental results. All interaction parameters are summarized in Table 1.

Figure 4 shows the measured cloud points and tie lines for $H_2O/HEC1/C_xE_{28}$. As in the theoretical example the tie lines run nearly parallel to the polymer/surfactant edge. The critical point is shifted towards a higher content of C_xE_{28}. The theoretical binodal line agrees well with the measured cloud points. Also the tie lines are well described within the experimental error. The coexisting phase where the surfactant is enriched contains nearly no HEC, whereas the other phase contains considerable amounts of C_xE_{28}. In Fig. 5 the phase diagram of the HEC of higher molar mass and the same surfactant as before is shown. The phase diagram is very similar to that of Fig. 4, the increase of M_{HEC} causes only a slight enlargement of the two-phase area. In the theoretical treatment polydispersity effects are neglected, nevertheless, the six adjustable parameters are sufficient to describe the real behavior. The same parameters also describe the phase diagram of the mixture with the HEC of the higher molar mass.

Applying the same interaction parameters to C_xE_{40} fails since the large micelles of this surfactant would cause a very small homogeneous region at the H_2O corner of the phase diagram. In this case the values of ω_{2u3p} and of

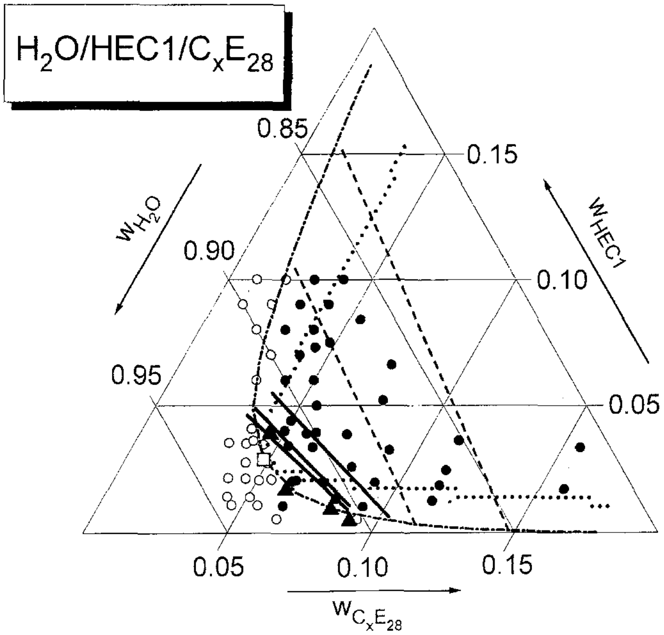

Fig. 4 Phase diagram of $H_2O/HEC1/C_xE_{28}$. Experimental data: heterogeneous (full circles) and homogeneous (open circles) area, cloud points (full triangles), and tie lines (full lines). Calculated data: tie lines (dashed), binodal (dash dotted) and spinodal line (dotted), and critical point (open square)

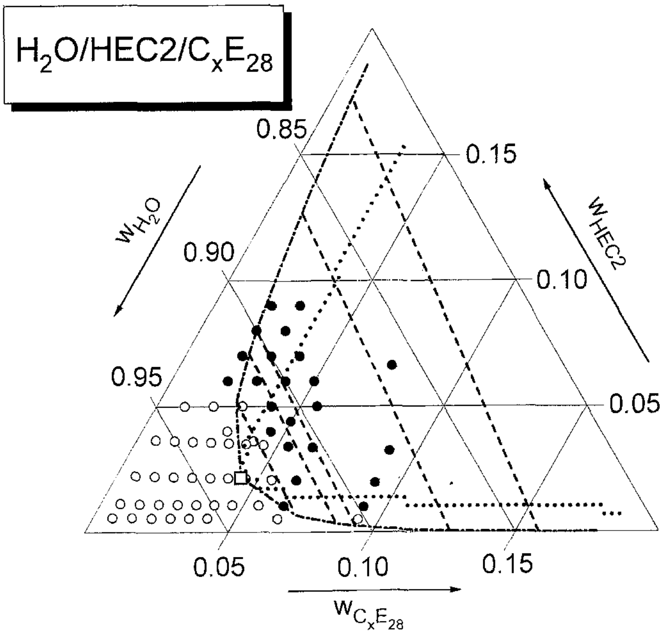

Fig. 5 Phase diagram of $H_2O/HEC2/C_xE_{28}$, data depicted as in Fig. 4

ω_{2p3u} are chosen to be slightly smaller (see Table 1). The change of these two interaction parameters only suffices to describe the phase diagram.

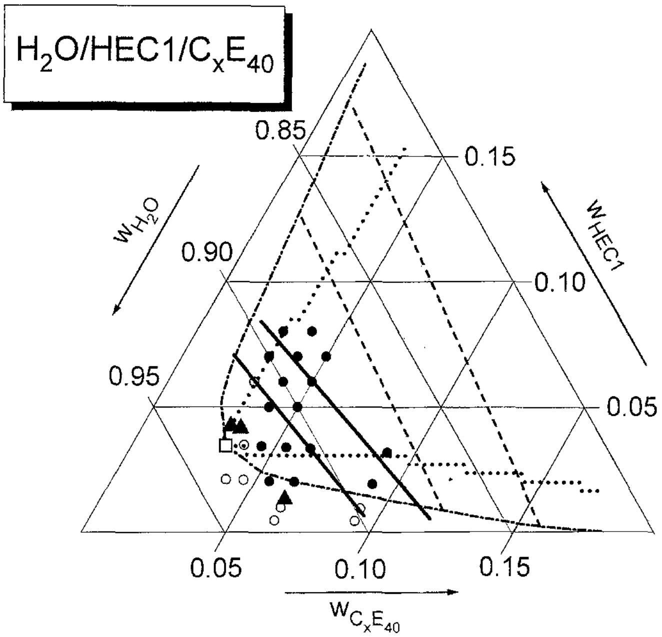

Fig. 6 Phase diagram of $H_2O/HEC/C_xE_{40}$, data depicted as in Fig. 4

The phase behavior of ternary aqueous solutions of two samples of hydroxyethyl cellulose (HEC) and oligoethylene glycol mono(*n*-alkyl) ethers C_xE_y ($y = 28, 40$) has been studied. The influence of molar mass of HEC and the number of ethylene glycol units on the phase behavior has been investigated. Both solutes are completely miscible with water. The mixture of water/polymer/nonionic surfactant phase separates segregatively, i.e., HEC is enriched in one phase, the surfactant in the other. The theoretical description is based on an equation for the Gibbs energy of mixing which takes polar conformations into account. The phase diagrams are calculated by means of a new method which does not require the derivatives of the Gibbs energy of mixing.

The phase diagrams of the three different ternary systems are very similar. Using the same surfactant and increasing the molar mass of HEC (Figs. 4 and 5) causes an enlargement of the heterogeneous region. Increasing the number of ethylene glycol units of the surfactant (i.e., enlargement of the hydrophilic part and simultaneously of the micelle size) mixed with HEC1 and water (Figs. 4 and 6) also extends the two-phase area. These experimental observations are in agreement with theoretical considerations.

Acknowledgments We would like to thank Mr. Horst Wurm for helpful discussions concerning the characterization of HEC and C_xE_y, as well as Dr. Otto Schönherr for the light scattering measurements, and Mrs. Kathrin Schellenberg for her experimental efforts. The financial support of the Deutsche Forschungsgemeinschaft (DFG) is gratefully acknowledged.

References

1. Chang Y, Lochhead RY, McCormick CL (1994) Macromolecules 27:2145
2. Loyen K, Iliopoulos I, Olsson U, Audebert R (1995) Progr Colloid Polym Sci 98:42
3. Walderhaug H, Nyström B, Hansen FK, Lindman B (1995) Progr Colloid Polym Sci 98:51
4. Kahlweit M, Strey R, Firman P, Haase D, Jen J, Schomäcker R (1988) Langmuir 4:499
5. Gradzielski M, Hoffmann H, Robisch P, Ulbricht W (1990) Tenside Deterg 27:366
6. Roberts GAF, Thomas IM (1978) Polymer 19:459
7. Kästner U, Hoffman H, Dönges R, Ehrler R (1995) Progr Colloid Polym Sci 98:57
8. Zhang K, Karlström G, Lindman B (1992) Colloids and Surfaces 67:147
9. Konigsveld R, Kleintjens LA (1988) Acta Polym 39:341
10. Einaga Y (1994) Progr Polym Sci 19:1
11. Karlström G (1985) J Phys Chem 89:4962
12. Brown W (Ed.) Dynamic Light Scattering, Clarendon Press, Oxford 1993
13. Chu B, Laser Light Scattering, Academic Press, London 1991
14. Flory JP, Principles of polymer chemistry, Cornell University Press, Ithaca NY, 1952
15. Zhang K, Karlström G, Lindman B (1994) J Phys Chem 98:4411
16. Horst R (1995) Macromol. Theory Simul 4:449
17. Horst R, Wolf BA (1996) Macromol Theory Simul 5:81
18. Picullell L, Lindmann B (1992) Adv Colloid Interface Sci 41:149
19. Huggins ML (1942) J Am Chem Soc 64:2716
20. Brown W, Henley D, Öhman J (1963) Makromol Chem 64:49
21. Wurm H, private communication